Delft University of Technology

Degradation modeling considering unit-to-unit heterogeneity-A general model and comparative study

Wang, Zhijie; Zhai, Qingqing; Chen, Piao

DOI
10.1016/j.ress.2021.107897

Publication date
2021

Document Version
Final published version

Published in
Reliability Engineering and System Safety

Citation (APA)
Wang, Z., Zhai, Q., & Chen, P. (2021). Degradation modeling considering unit-to-unit heterogeneity-A general model and comparative study. *Reliability Engineering and System Safety*, *216*, Article 107897. https://doi.org/10.1016/j.ress.2021.107897

Important note
To cite this publication, please use the final published version (if applicable).
Please check the document version above.

Copyright
Other than for strictly personal use, it is not permitted to download, forward or distribute the text or part of it, without the consent of the author(s) and/or copyright holder(s), unless the work is under an open content license such as Creative Commons.

Takedown policy
Please contact us and provide details if you believe this document breaches copyrights.
We will remove access to the work immediately and investigate your claim.

This work is downloaded from Delft University of Technology.
For technical reasons the number of authors shown on this cover page is limited to a maximum of 10.

Green Open Access added to TU Delft Institutional Repository

'You share, we take care!' - Taverne project

https://www.openaccess.nl/en/you-share-we-take-care

Otherwise as indicated in the copyright section: the publisher is the copyright holder of this work and the author uses the Dutch legislation to make this work public.

Reliability Engineering and System Safety 216 (2021) 107897

Contents lists available at ScienceDirect

Reliability Engineering and System Safety

journal homepage: www.elsevier.com/locate/ress

Degradation modeling considering unit-to-unit heterogeneity-A general model and comparative study

Zhijie Wang [a], Qingqing Zhai [a,*], Piao Chen [b]

[a] School of Management, Shanghai University, Shanghai, China
[b] Delft Institute of Applied Mathematics, Delft University of Technology, Netherlands

ARTICLE INFO

Keywords:
Heterogeneous degradation
Generalized inverse Gaussian distribution
Wiener process model
EM algorithm

ABSTRACT

The performance of units in the same batch can exhibit considerable heterogeneity due to the variation in the raw materials and fluctuation in the manufacturing process. For products suffering performance degradation in their use, such heterogeneity often results in an increase in the dispersion of the degradation paths of units in a population. The degradation rate of products can be unit-specific and often treated as random effects. This paper develops a novel random-effects Wiener process model to account for the unit-to-unit heterogeneity in the degradation, where the generalized inverse Gaussian (GIG) distribution is used to model the unit-specific degradation rate. The GIG distribution is a very general distribution with broad applications, which includes the inverse Gaussian (IG) distribution and the Gamma distribution as special cases. We investigate the model properties and develop an expectation maximization (EM) algorithm for parameter estimation. By comparing the proposed model with existing models on two real degradation datasets of the infrared LEDs and the GaAs lasers, we show that the proposed model is quite effective for degradation modeling with heterogeneous rates.

Notations

$X(t)$ Degradation level at time t
$\Lambda(t;\theta)$ Time scale transformation function with parameter θ
$\mathscr{B}(\cdot)$ Standard Brownian motion
v Drift rate
D_f Predetermined failure threshold
T_f First passage time of $X(t)$ with respect to D_f
$\Gamma(\cdot)$ Gamma function
$\mathscr{K}_p(\cdot)$ Modified Bessel function of the second kind
$\mathscr{N}(\cdot)$ Gaussian distribution
$\mathrm{E}[\bullet]$ Expectation operator
$\mathrm{Var}[\bullet]$ Variance operator
n Number of units of a degradation dataset
m_i Number of degradation observations for unit $i, i = 1, \ldots, n$
$t_{i,j}$ The jth condition monitoring time of unit i, $j = 1, \ldots, m_i$
$X_{i,j}$ The jth degradation observation of unit i at $t_{i,j}$
$X_i = \{X_{i,1}, \cdots, X_{i,m_i}\}$ Degradation observations for unit i
$\mathbf{X} = \{X_1, \cdots, X_n\}$ Degradation observations for the n units
$\mathbf{V} = \{v_1, \cdots, v_n\}$ Drift of the n units
$\mathbf{\Theta}$ Unknown model parameters
$\mathbf{\Theta}^{(k)}$ Estimated $\mathbf{\Theta}$ at the kth step in the EM algorithm
$\ell(\mathbf{\Theta}|\mathbf{X})$ Log-likelihood for degradation data $\mathbf{X}$
$\ell(\mathbf{\Theta}|\mathbf{V},\mathbf{X})$ Complete log-likelihood for the complete data $\{\mathbf{V}, \mathbf{X}\}$
$Q(\mathbf{\Theta}|\mathbf{\Theta}^{(k-1)})$ Expectation of $\ell(\mathbf{\Theta}|\mathbf{V},\mathbf{X})$ with respect to the conditional distribution of $\mathbf{V}$ given $\mathbf{X}$ and $\mathbf{\Theta}^{(k-1)}$

1. Introduction

In many industrial applications, the quality characteristics of devices and systems would degrade over time. For instance, the lumen output of LED decreases with usage [1], and mechanical parts such as bearings often wear gradually with an increase in vibration and noise [2]. When the degradation level exceeds an admissible or safe threshold, the system is deemed failed. To predict the failure time and assess the reliability of systems, it is of importance to monitor these performance indicators and model the degradation process. Once the degradation model is available, the remaining useful life of the system can be established. Subsequently, effective maintenance actions, such as repair and replacement, can be arranged to avoid unexpected sudden failures, and the lifecycle cost can be optimized [3].

Many approaches have been proposed for degradation modeling,

* Corresponding author.
E-mail address: zhaiq@shu.edu.cn (Q. Zhai).

https://doi.org/10.1016/j.ress.2021.107897
Received 24 March 2021; Received in revised form 1 July 2021; Accepted 2 July 2021
Available online 13 July 2021
0951-8320/© 2021 Elsevier Ltd. All rights reserved.

including the general path models, the stochastic process models, and the machine learning-based models. The general path models assume the degradation trajectories can be fitted by deterministic functions, which overlook the temporal uncertainties in the degradation process [4]. The machine learning-based models, such as the support vector machine [5] and deep learning approaches [6], are heavily dependent on the training dataset, which may be insufficient in engineering practice. Stochastic process models take the temporal randomness of the degradation process into account, which are especially favored for degradation modeling in recent years [7-9]. Commonly-used stochastic process models include the Wiener process [10-13], the Gamma process [14] and the inverse Gaussian process [15,16]. The Gamma process and the inverse Gaussian process are monotone, and they are widely used to model degradation with monotonic paths, such as crack growth and wearing. On the other hand, the Wiener process can model non-monotone degradation paths, and it has been successfully applied to the degradation modeling of rail tracks [17], lithium-ion batteries [18], LEDs [19], electrical distribution devices [20] and many other products [21].

Traditional Wiener process models assume that the units from a same batch are homogeneous. Due to the variation in the raw materials and fluctuation in the manufacturing process, however, units from a same batch may exhibit considerable heterogeneity in their degradation paths. Such heterogeneity is often modeled as random-effects, where some degradation characteristics, such as the degradation rate, are assumed to be unit-specific and random in the population. For Wiener process models, the normal distribution is widely adopted to describe the heterogeneous degradation rate for mathematical convenience [22, 23]. Sun et al. [24] considered the accelerated degradation test and used a Wiener process model with normally distributed degradation rates to account for the heterogeneity in the population. Xu et al. [25] also applied the Wiener process with normal random-effects to model the degradation of lithium-ion batteries. Wang [26] considered the heterogeneity in the diffusion coefficient of the Wiener process, where the diffusion coefficient follows an inverse Gamma distribution and the drift rate follows a normal distribution conditional on the diffusion coefficient. Ye et al. [27] assumed a normal distribution for the reciprocal of the drift rate parameter and incorporated the heterogeneity of the diffusion coefficient using a linear relationship between the drift rate and the diffusion coefficient.

The Wiener process model with normal random-effects is convenient and have attracted lots of attentions, yet using the normal distribution for the heterogeneous degradation rate has certain shortcomings. One deficiency lies in that the degradation rate is generally one-sided (positive or negative), but the normal distribution has a support on the whole real domain. Although the probability of the negative part is negligible when the expectation is larger than three times of the standard deviation, it is only approximately true and depends on the distribution parameters [27]. The truncated normal distribution can remedy this deficiency, but it also complicates the model [28]. In addition, the normal distribution has a symmetric probability density function (PDF), which is restricted in applications when the heterogeneous degradation rate follows skewed distributions. For example, it is observed that a skewed distribution is more suitable for the heterogeneous degradation rate of the laser devices [29]. In addition, the typical Wiener process with normally distributed drift also overlooks the heterogeneous in the volatility of the degradation process. Zhai et al. [29] fitted each path in a GaAs laser device degradation dataset using the traditional Wiener process model, and found that there exists positive correlation between the degradation rate and the diffusion coefficient. Yan et al. [30] used the same method to study a silicon rubber aging dataset, and arrived at a similar conclusion. Therefore, it is also necessary to take into account the heterogeneity in the diffusion coefficient in degradation modeling of heterogeneous populations.

To address these concerns, a novel Wiener process considering the heterogeneity in the population is proposed in this paper. We exploit the accelerated failure time concept to link the degradation rate and the diffusion coefficient, by which the heterogeneity in the degradation process can be fully accounted for. Further, the unit-specific degradation rate is characterized by a generalized inverse Gaussian (GIG) distribution, which has a positive support and overcomes the deficiencies of the normal distribution as the random-effects. The proposed model generalizes some existing models, e.g. the model in [29], and also induces some new special models due to the generality of the GIG distribution. The proposed model is analytically tractable and an EM algorithm is developed for model parameter estimation. The performance is compared with existing models by the application to two real degradation datasets, and its applicability in degradation modeling is discussed. To sum up, the paper contributes to the study on degradation modeling in two folds:

- First, we propose a general family of Wiener process models with GIG distributed random effects for heterogeneous population, and the estimation procedure is developed.
- Second, a comprehensive comparative study is implemented for the proposed models with the existing models, by which the applicability of the proposed model is validated.

The remainder of the paper is organized as follows. Section 2 gives the detailed model formulation and the model properties. In Section 3, the EM algorithm is developed to implement the maximum likelihood estimation (MLE) of the proposed model. Section 4 implements comparative study based on two degradation datasets to compare the proposed model with existing ones. Conclusions are given in Section 5.

2. Wiener process model with GIG random-effects

2.1. The model formulation

The Wiener process is one of the most popular degradation models in recent years [10,18,19,29]. In this study, we consider the Wiener process model with the following form:

$$X(t) = \nu\Lambda(t) + \kappa\mathscr{B}(\nu\Lambda(t)), \tag{1}$$

where $\nu > 0$ is the drift rate, $\kappa > 0$ is the diffusion parameter, and $\mathscr{B}(\cdot)$ represents a standard Brownian motion. The transformed time scale $\Lambda(t) = \Lambda(t;\ \theta)$ with parameter θ is used to capture possible non-linear degradation patterns. Following the convention, it is assumed that $\Lambda(t)$ is monotonically increasing with $\Lambda(0) = 0$. For instance, $\Lambda(t)$ can follow the power law form $\Lambda(t) = t^{\theta}$.

The model in (1) was originally proposed in [29] based on the accelerated failure time model (AFTM). In accelerated test, the elevated stress can lead to a shortened lifetime of product, and this effect can be modeled by scaling of the time scale under the normal stress in the AFTM. Following the same idea, the heterogeneity in the degradation of a population can be modeled as a random scaling effect of the time scale. More specifically, ν can be seen as the scaling factor that reflects the randomness in the quality of the unit and the randomness from the operating environment. The degradation pattern for the population is identical, which is modeled as a Wiener process, while the time scale $\nu\Lambda(t)$ is unit-specific.

In model (1), the degradation rate and the diffusion are ν and $\kappa^2\nu$, respectively. This indicates that the magnitude of the fluctuations in the degradation path is dependent on the particular degradation rate ν, which explains a common phenomenon in degradation data that the unit with a larger degradation rate often has a larger variation.

To capture the heterogeneity in a population, ν is assumed to follow a GIG distribution $\mathscr{GIG}(a, b, p)$ with the following PDF:

$$f(\nu) = \frac{(a/b)^{\frac{p}{2}}}{2\mathscr{K}_p\left(\sqrt{ab}\right)}\nu^{p-1}\exp\left(-\frac{1}{2}\left(a\nu + b\nu^{-1}\right)\right),\ \ \nu > 0 \tag{2}$$

where $a > 0$, $b > 0$, $p \in (-\infty, +\infty)$ and

$$\mathscr{K}_p(z) = \frac{1}{2}\int_0^{+\infty} y^{p-1}\exp\left(-\frac{z}{2}\left(y + y^{-1}\right)\right)dy \tag{3}$$

is the modified Bessel function of the second kind [31]. The GIG distribution is a generalization of the inverse Gaussian distribution, which has been widely applied in industrial applications [32]. In particular, the GIG distribution degenerates to the inverse Gaussian distribution if the parameter p is fixed to $-1/2$. In addition, the GIG distribution also generalizes the Gamma distribution, and it degenerates to the Gamma distribution when the parameter b approaches 0.

Conditional on the degradation rate v, the degradation $X(t)$ at any time t follows the following normal distribution:

$$X(t)|v \sim \mathscr{N}\left(v\Lambda(t), v\kappa^2\Lambda(t)\right). \tag{4}$$

Consequently, the unconditional distribution of $X(t)$ can be obtained by integrating v out. Based on (2) and (4), the unconditional PDF of $X(t)$ can be obtained as

$$f_{X(t)}x = \int_0^{+\infty} \frac{1}{\sqrt{2\pi\kappa^2 v\Lambda(t)}}\exp\left(-\frac{(x - v\Lambda(t))^2}{2\kappa^2 v\Lambda(t)}\right)\frac{\left(\frac{a}{b}\right)^{\frac{p}{2}}}{2\mathscr{K}_p\left(\sqrt{ab}\right)}v^{p-1}\exp\left(-\frac{1}{2}\left(av + bv^{-1}\right)\right)dv = \frac{1}{\sqrt{2\pi\kappa^2\Lambda(t)}}\frac{(a/b)^{\frac{p}{2}}}{\mathscr{K}_p\left(\sqrt{ab}\right)}\exp\left(\frac{x}{\kappa^2}\right)\mathscr{K}_{p-\frac{1}{2}}\left(\sqrt{A(t)B(t)}\right)\left(\frac{B(t)}{A(t)}\right)^{\frac{\left(p-\frac{1}{2}\right)}{2}} \tag{5}$$

where

$$A(t) = a + \frac{\Lambda(t)}{\kappa^2},\; B(t) = \frac{x^2}{\kappa^2\Lambda(t)} + b. \tag{6}$$

The unconditional expectation and variance of $X(t)$ can be obtained as:

$$\mathrm{E}[X(t)] = \mathrm{E}[v]\Lambda(t),\; \mathrm{Var}[X(t)] = \mathrm{Var}[v]\Lambda^2(t) + \kappa^2\mathrm{E}[v]\Lambda(t). \tag{7}$$

The expectation and variance of a GIG random variable can be expressed in terms of the modified Bessel function of the second kind [31]:

$$\mathrm{E}[v] = \frac{\sqrt{b}\mathscr{K}_{p+1}\left(\sqrt{ab}\right)}{\sqrt{a}\mathscr{K}_p\left(\sqrt{ab}\right)},\; \mathrm{Var}[v] = \frac{b\mathscr{K}_{p+2}\left(\sqrt{ab}\right)}{a\mathscr{K}_p\left(\sqrt{ab}\right)} - \mathrm{E}[v]^2. \tag{8}$$

2.2. Reliability analysis based on the proposed model

For products suffering degradation, its lifetime is often defined as the first hitting time of $X(t)$ with respect to a predetermined threshold D_f: $T_f = inf\{t : X(t) > D_f\}$. The product is deemed failed if the degradation exceeds the threshold and should be repaired or replaced. Conditional on v, $X(t)$ has a linear degradation path under the transformed time scale $\Lambda(t)$, and the first hitting time under $\Lambda(t)$ follows an IG distribution, i.e., $\Lambda(T_f) \sim \mathscr{IG}\left(\frac{D_f}{v}, \frac{D_f^2}{v\kappa^2}\right)$. More specifically, the PDF of the conditional distribution of $\Lambda(T_f)$ is:

$$f_{\Lambda(T_f)|v}(u) = \sqrt{\frac{D_f^2}{2\pi v\kappa^2 u^3}}\exp\left(-\frac{v\left(u - \frac{D_f}{v}\right)^2}{2\kappa^2 u}\right). \tag{9}$$

The PDF of $\Lambda(T_f)$ can be obtained by integrating v out:

$$f_{\Lambda(t)}(u) = \sqrt{\frac{D_f^2}{2\pi\kappa^2 u^3}}\;\frac{\left(\frac{a}{b}\right)^{\frac{p}{2}}}{\mathscr{K}_p\left(\sqrt{ab}\right)}\exp\left(\frac{D_f}{\kappa^2}\right)\cdot\mathscr{K}_{p-\frac{1}{2}}\left(\sqrt{\left(a + \frac{u}{\kappa^2}\right)\left(\frac{D_f^2}{\kappa^2 u} + b\right)}\right)\left(\frac{D_f^2 + b\kappa^2 u}{u^2 + a\kappa^2 u}\right)^{\frac{\left(p-\frac{1}{2}\right)}{2}}. \tag{10}$$

Given that $\Lambda(t)$ is differentiable, the PDF of T_f under the calendar time t is

$$f_{T_f}(t) = f_{\Lambda(T_f)}(\Lambda(t))\frac{d\Lambda(t)}{dt}. \tag{11}$$

The expected lifetime of the degradation unit can be derived based on $f_{T_f}(t)$. For example, if the transformed time scale follows the power law form $\Lambda(t) = t^\theta$, then the mean and variance of T_f can be derived as

$$\mathrm{E}\left[T_f\right] = \sqrt{\frac{2D_f}{\pi\kappa^2}}\exp\left(\frac{D_f}{\kappa^2}\right)D_f^{\frac{1}{\theta}}\frac{\mathscr{K}_{p-\frac{1}{\theta}}\left(\sqrt{ab}\right)\mathscr{K}_{-\frac{1}{2}+\frac{1}{\theta}}\left(\frac{D_f}{\kappa^2}\right)}{\mathscr{K}_p\left(\sqrt{ab}\right)}\frac{a}{b}^{\frac{1}{2\theta}}, \tag{12}$$

$$\mathrm{Var}\left[T_f\right] = \sqrt{\frac{2D_f}{\pi\kappa^2}}\exp\left(\frac{D_f}{\kappa^2}\right)D_f^{\frac{2}{\theta}}\frac{\mathscr{K}_{p-\frac{2}{\theta}}\left(\sqrt{ab}\right)\mathscr{K}_{-\frac{1}{2}+\frac{2}{\theta}}\left(\frac{D_f}{\kappa^2}\right)}{\mathscr{K}_p\left(\sqrt{ab}\right)}\frac{a}{b}^{\frac{1}{\theta}} - \mathrm{E}\left[T_f\right]^2. \tag{13}$$

The establishment of the first hitting time T_f is an important part in the prognostics and health management. Once the PDF of T_f is obtained based on the above inference, the expected lifetime of the in-service systems can be estimated with a predetermined threshold D_f. Then, appropriate health management works can be performed to ensure the reliability and stability of industrial devices.

2.3. Gamma distribution as a special case of the GIG distribution

As mentioned in Section 2.1, the GIG distribution degenerates to the

Gamma distribution if b approaches 0. As a special case of the GIG distribution, the Gamma distribution is also utilized widely in engineering field. When the proposed model has the Gamma random-effects, the unconditional PDF of the degradation $X(t)$ is

$$\begin{aligned} f_{X(t)}x &= \int_0^{+\infty} \frac{1}{\sqrt{2\pi\kappa^2 v\Lambda(t)}} \exp\left(-\frac{(x-v\Lambda(t))^2}{2\kappa^2 v\Lambda(t)}\right) \frac{1}{\Gamma(p)}\left(\frac{a}{2}\right)^p \\ & v^{p-1}\exp\left(-\frac{1}{2}av\right)dv \\ &= \frac{1}{\sqrt{2\pi\kappa^2 v\Lambda(t)}}\frac{1}{\Gamma(p)}\frac{a^p}{2^{p-1}}\exp\left(\frac{x}{\kappa^2}\right)\mathscr{K}_p\left(\sqrt{\frac{x^2}{\kappa^2\Lambda(t)}\left(a+\frac{\Lambda(t)}{\kappa^2}\right)}\right) \\ & \left(\frac{x^2}{\Lambda(t)^2 + a\kappa^2\Lambda(t)}\right)^{\frac{p}{2}}. \end{aligned} \tag{14}$$

Accordingly, we can also derive the PDF of the first hitting time $\Lambda(T_f)$ under the time scale $\Lambda(\cdot)$ as:

$$\begin{aligned} f_{\Lambda(T_f)}(u) &= \sqrt{\frac{D_f^2}{2\pi\kappa^2 u^3}}\frac{\left(\frac{a}{2}\right)^{\frac{p}{2}}}{\Gamma(p)}\exp\left(\frac{D_f}{\kappa^2}\right) \\ & \mathscr{K}_{p-\frac{1}{2}}\left(\sqrt{\left(a+\frac{u}{\kappa^2}\right)\frac{D_f^2}{\kappa^2 u}}\right)\left(\frac{D_f^2}{u^2+a\kappa^2 u}\right)^{\left(p-\frac{1}{2}\right)\Big/2}. \end{aligned} \tag{15}$$

When the time scale transformation function follows the power law form $\Lambda(t) = t^\theta$, the expectation and the variance of T_f are

$$\mathrm{E}[T_f] = \sqrt{\frac{2D_f}{\pi\kappa^2}}\exp\left(\frac{D_f}{\kappa^2}\right)D_f^{\frac{1}{\theta}}\mathscr{K}_{-\frac{1}{2}+\frac{1}{\theta}}\left(\frac{D_f}{\kappa^2}\right)\frac{\Gamma\left(p-\frac{1}{\theta}\right)}{\Gamma(p)}\left(\frac{a}{2}\right)^{\frac{1}{\theta}-\frac{p}{2}}, \tag{16}$$

$$\mathrm{Var}[T_f] = \sqrt{\frac{2D_f}{\pi\kappa^2}}\exp\left(\frac{D_f}{\kappa^2}\right)D_f^{\frac{2}{\theta}}\mathscr{K}_{-\frac{1}{2}+\frac{2}{\theta}}\left(\frac{D_f}{\kappa^2}\right)\frac{\Gamma\left(p-\frac{2}{\theta}\right)}{\Gamma(p)}\left(\frac{a}{2}\right)^{\frac{2}{\theta}-\frac{p}{2}} - \mathrm{E}[T_f]^2. \tag{17}$$

Thus, the reliability analysis based on the proposed model with GIG distributed random-effects and its special case with Gamma distributed random-effects is analytically tractable. For the special case with IG distributed random-effects, the corresponding reliability analysis can be seen in [29]. As stated above, the proposed model with GIG distributed random-effects includes the one with Gamma random-effects and with IG random-effects as special cases, which provides more flexibility for degradation modeling while maintains the mathematical convenience.

3. Parameter estimation with EM algorithm

In this section, the parameter estimation for the proposed model is discussed. Suppose that we have collected the degradation observations of unit i at m_i discrete time points $(t_{i,1}, \dots, t_{i,m_i})$ for $i = 1, \cdots, n$ in a degradation test. Denote $X_{i,j} = X(t_{i,j})$ as the degradation record at time $t_{i,j}$, $\boldsymbol{X}_i = (X_{i,1}, \dots, X_{i,m_i})^{\mathrm{T}}$ as the degradation record for unit i, and $\mathbf{X} = \{\boldsymbol{X}_1, \cdots, \boldsymbol{X}_n\}$ as the degradation data of the n units, where the superscript "T" denotes matrix transposition.

Let $\Delta X_{i,j} = X_{i,j} - X_{i,j-1}$ with $X_{i,0} = 0$. According to the property of the Wiener process, the increments $\Delta X_{i,j}, j = 1, \dots, m_i$ are independent and follow the normal distribution conditional on the drift rate v:

$$(\Delta X_{i,j}|v_i) \sim \mathscr{N}(v_i\Delta\Lambda_{i,j},\ v_i\kappa^2\Delta\Lambda_{i,j}), \tag{18}$$

where $\Delta\Lambda_{i,j} = \Lambda(t_{i,j}) - \Lambda(t_{i,j-1}),\ j = 1, \dots, m_i$. By convention, let $t_{i,0} = 0$. Accordingly, the joint distribution of $\boldsymbol{X}_i$ conditional on v_i is normal with the following PDF:

$$\begin{aligned} p(\boldsymbol{X}_i|v_i) &= \prod_{j=1}^{m_i} p(\Delta X_{i,j}\ |v_i) \\ &= \prod_{j=1}^{m_i}\frac{1}{\sqrt{2\pi v_i\kappa^2\Delta\Lambda_{i,j}}}\exp\left(-\frac{(\Delta X_{i,j} - v_i\Delta\Lambda_{i,j})^2}{2v_i\kappa^2\Delta\Lambda_{i,j}}\right). \end{aligned} \tag{19}$$

Unconditionally, the joint distribution of $\boldsymbol{X}_i$ can be obtained as

$$\begin{aligned} p(\boldsymbol{X}_i) &= \int_0^{+\infty} p(\boldsymbol{X}_i|v_i)f(v_i)dv_i \\ &= \sqrt{\frac{1}{(2\pi)^{m_i}\kappa^{2m_i}}}\prod_{j=1}^{m_i}\frac{1}{\sqrt{\Delta\Lambda_{i,j}}}\exp\left(\frac{X_{i,m_i}}{\kappa^2}\right)\frac{\left(\frac{a}{b}\right)^{\frac{p}{2}}}{\mathscr{K}_p\left(\sqrt{ab}\right)} \\ & \mathscr{K}_{P_i}\left(\sqrt{A_iB_i}\right)\left(\frac{B_i}{A_i}\right)^{P_i/2} \end{aligned} \tag{20}$$

where

$$A_i = a + \frac{\Lambda_{i,m_i}}{\kappa^2},\ B_i = b + \frac{1}{\kappa^2}\sum_{j=1}^{m_i}\frac{\Delta X_{i,j}^2}{\Delta\Lambda_{i,j}},\ P_i = p - \frac{m_i}{2} \tag{21}$$

The unknown model parameters involve the parameters in the GIG random-effects $\{a, b, p\}$, the diffusion coefficient κ^2 and the possible parameters in θ in the time scale transformation function $\Lambda(t;\theta)$. Denote $\boldsymbol{\Theta} = \{a,\ b,\ p,\ \kappa^2,\ \theta\}$. Based on the observed degradation data, the maximum likelihood (ML) estimates for the model parameters can be obtained by maximizing the following log-likelihood function:

$$\ell(\boldsymbol{\Theta}\mathrm{X}) = \sum_{i=1}^{n}\ln\ p(\boldsymbol{X}_i|\boldsymbol{\Theta}). \tag{22}$$

Referring to (20), we can see that the model parameters are involved in the modified Bessel function $\mathscr{K}$, which causes difficulties in directly maximizing the log-likelihood function. To address this problem, we treat the unit-specific drift rate as the latent variable, and resort to the EM algorithm to obtain the ML estimates.

3.1. The EM algorithm

Denote $\mathbf{V} = (v_1, \cdots, v_n)^{\mathrm{T}}$. By treating the unobserved drift rates of the n units as missing data, the complete log-likelihood for the complete data $\{\mathbf{V}, \mathbf{X}\}$ can be obtained as

$$\ell(\boldsymbol{\Theta}\mathrm{X}, \boldsymbol{V}) = \ell_V + \ell_X, \tag{23}$$

where

$$\begin{aligned} \ell_V &= \sum_{i=1}^{n}\ln f(v_i) \\ &= -n\ln\left[2\mathscr{K}_p\left(\sqrt{ab}\right)\right] + \frac{np}{2}\ln a - \frac{np}{2}\ln b + (p-1)\sum_{i=1}^{n}\ln v_i \\ & -\frac{1}{2}\sum_{i=1}^{n}\left(av_i + bv_i^{-1}\right), \end{aligned} \tag{24}$$

$$\begin{aligned} \ell_X &= \sum_{i=1}^{n}\ln p(\boldsymbol{X}_i|v_i, \boldsymbol{\Theta}) \\ &= \sum_{i=1}^{n}\left\{-\frac{m_i}{2}\ln(2\pi) - \frac{m_i}{2}\ln\left[\kappa^2 v_i\right] - \frac{1}{2}\sum_{j=1}^{m_i}\ln\Delta\Lambda_{i,j} - \frac{1}{2\kappa^2 v_i}\sum_{j=1}^{m_i}\frac{(\Delta X_{i,j} - v_i\Delta\Lambda_{i,j})^2}{\Delta\Lambda_{i,j}}\right\} \end{aligned} \tag{25}$$

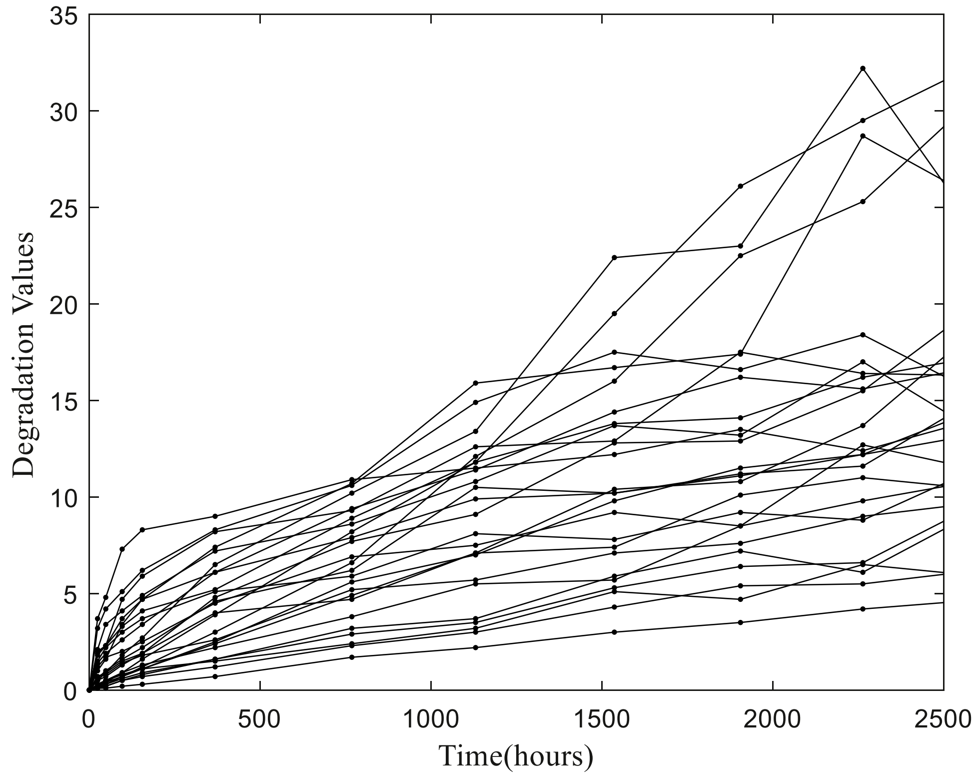

Fig. 1. Degradation paths of 25 IRLEDs.

The EM algorithm is an iterative algorithm, where each iteration implements the expectation-step (E-step) and maximization-step (M-step). In the kth iteration of the EM algorithm, the E-step calculates the expectation of the complete log-likelihood with respect to the conditional distribution of the mission data $\mathbf{V}$ given the observation X, i.e., $p(\mathbf{V}|\mathbf{X}, \mathbf{\Theta}^{(k-1)})$, where $\mathbf{\Theta}^{(k-1)}=\{a^{(k-1)},b^{(k-1)},p^{(k-1)},[\kappa^{(k-1)}]^2,\theta^{(k-1)}\}$ denotes the estimates for the model parameters in the last iteration. More specifically, the E-step derives the following Q-function:

$$Q\left(\mathbf{\Theta}\middle|\mathbf{\Theta}^{(k-1)}\right) = E_{\mathbf{V}|\mathbf{X},\mathbf{\Theta}^{(k-1)}}[\ell(\mathbf{\Theta}|\mathbf{V},\mathbf{X})] \tag{26}$$

After the Q-function is obtained, the estimates for the model parameters are updates by maximizing the Q-function with respect to $\mathbf{\Theta}$:

$$\mathbf{\Theta}^{(k)} = \text{argmax}_{\mathbf{\Theta}} Q\left(\mathbf{\Theta}\middle|\mathbf{\Theta}^{(k-1)}\right). \tag{27}$$

To accomplish this, we first treat the parameters p and θ as fixed. By deriving the first order partial derivatives of $Q(\mathbf{\Theta}|\mathbf{\Theta}^{(k)})$ with respect to a, b and κ^2 and letting them equal to zero, we have

$$2pn - 2a\sum_{i=1}^{n} E_{\mathbf{V}|\mathbf{X},\mathbf{\Theta}^{(k-1)}}[v_i] + \frac{n\sqrt{ab}}{\mathscr{K}_p(\sqrt{ab})}\left\{\mathscr{K}_{p+1}\left(\sqrt{ab}\right) + \mathscr{K}_{p-1}\left(\sqrt{ab}\right)\right\} = 0, \tag{28}$$

$$2pn + 2b\sum_{i=1}^{n} E_{\mathbf{V}|\mathbf{X},\mathbf{\Theta}^{(k-1)}}\left[v_i^{-1}\right] - \frac{n\sqrt{ab}}{\mathscr{K}_p(\sqrt{ab})}\left\{\mathscr{K}_{p+1}\left(\sqrt{ab}\right) + \mathscr{K}_{p-1}\left(\sqrt{ab}\right)\right\} = 0, \tag{29}$$

$$\kappa^2 = \frac{1}{n\sum_{i=1}^{n} m_i}\sum_{i=1}^{n}\left\{\Lambda_{i,m_i}E_{\mathbf{V}|\mathbf{X},\mathbf{\Theta}^{(k-1)}}[v_i] - 2X_{i,m} + \left[\sum_{j=1}^{m_i}\frac{\Delta X_{i,j}^2}{\Delta\Lambda_{i,j}}\right]E_{\mathbf{V}|\mathbf{X},\mathbf{\Theta}^{(k-1)}}\left[v_i^{-1}\right]\right\}. \tag{30}$$

Combining the first two equations yields

$$a = \frac{2pn + b\sum_{i=1}^{n} E_{\mathbf{V}|\mathbf{X},\mathbf{\Theta}^{(k-1)}}\left[v_i^{-1}\right]}{\sum_{i=1}^{n} E_{\mathbf{V}|\mathbf{X},\mathbf{\Theta}^{(k-1)}}[v_i]}. \tag{31}$$

Then, substituting (31) into (29) and solving it with respect to b, we can get the estimate for b. Subsequently, the estimates for a and κ^2 can be obtained by substituting the estimated b back to (31) and (30), respectively. The estimates $\{\widehat{a}, \widehat{b}, \widehat{\kappa}^2\}$ are obtained for each fixed $\{p,\theta\}$, which are functions of $\{p,\theta\}$. Substituting $\{\widehat{a}, \widehat{b}, \widehat{\kappa}^2\}$ back into $Q(\mathbf{\Theta}|\mathbf{\Theta}^{(k-1)})$, we obtain the profiled Q-function as a function of $\{p,\theta\}$:

$$\widetilde{Q}(p,\theta) = Q\left(\widehat{a}(p,\theta), \widehat{b}(p,\theta), \widehat{\kappa}(p,\theta)^2, p, \theta\middle|\mathbf{\Theta}^{(k-1)}\right) \tag{32}$$

The estimates for $\{p,\theta\}$ is obtained by maximizing the profiled Q-function with respect to p and θ. The EM algorithm iterates until the difference between the estimates for the model parameters in two consecutive iterations is smaller than a given threshold, and the ML estimates for $\mathbf{\Theta}$ is obtained.

3.2. E-step in the EM algorithm

As can be noticed, we have to calculate the expectation of v_i and v_i^{-1} with respect to the conditional distribution $p(\mathbf{V}|\mathbf{X}, \mathbf{\Theta}^{(k-1)})$. The conditional distribution $p(VX)$ can obtained as

$$p(\mathbf{V}|\mathbf{X}) \propto p(\mathbf{V},\mathbf{X}) = \prod_{i=1}^{n} f(v_i)p(\boldsymbol{X}_i|v_i), \tag{33}$$

which means that the conditional distribution $p(\mathbf{V}|\mathbf{X})$ can be decomposed as

$$p(\mathbf{V}|\mathbf{X}) = \prod_{i=1}^{n} p(v_i|\boldsymbol{X}_i), \tag{34}$$

where $p(v_i|\boldsymbol{X}_i)$ is obtained as

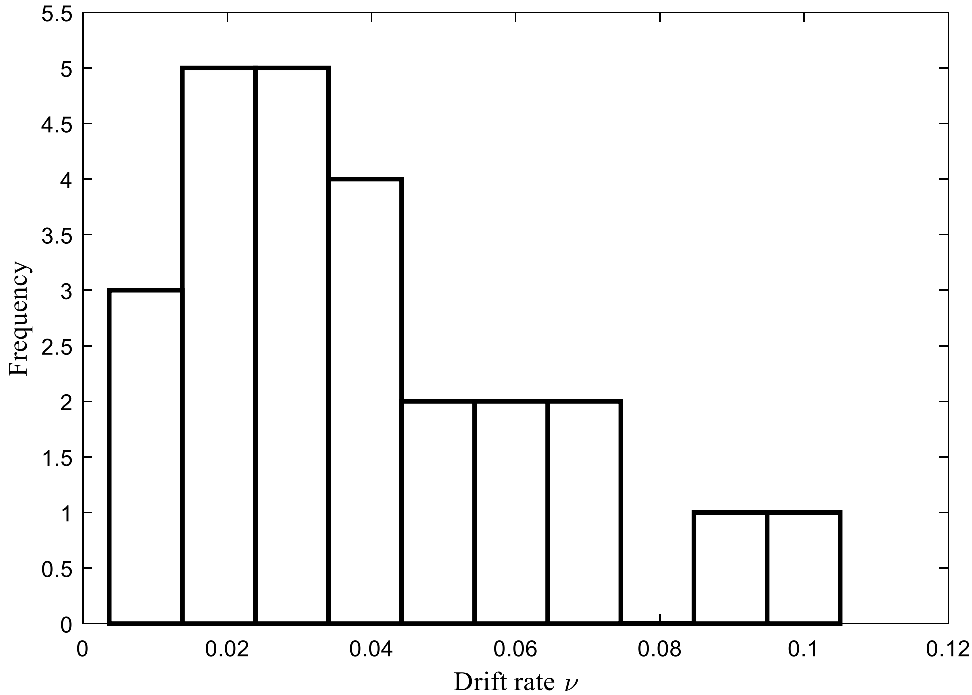

Fig. 2. Histogram of the drift rates of 25 IRLEDs when fitting each path individually by the basic Wiener process.

$$p(v_i|\boldsymbol{X}_i) = \frac{f(v_i)p(\boldsymbol{X}_i|v_i)}{p(\boldsymbol{X}_i)} = \frac{(A_i/B_i)^{P_i/2}}{2\mathscr{K}_{P_i}\left(\sqrt{A_iB_i}\right)} v_i^{P_i-1}\exp\left(-\frac{1}{2}\left(A_iv_i + B_iv_i^{-1}\right)\right). \tag{35}$$

Formula (35) indicates that the distribution of v_i conditional on the degradation observations X_i also follows a GIG distribution with parameters (A_i, B_i, P_i). According to the properties of the GIG distribution [32], it can be readily obtained that

$$E_{\mathbf{V}|\mathbf{X},\boldsymbol{\Theta}^{(k-1)}}[v_i] = \frac{\sqrt{B_i}\mathscr{K}_{P_i+1}\left(\sqrt{A_iB_i}\right)}{\sqrt{A_i}\mathscr{K}_{P_i}\left(\sqrt{A_iB_i}\right)}, \tag{36}$$

$$E_{\mathbf{V}|\mathbf{X},\boldsymbol{\Theta}^{(k-1)}}\left[v_i^{-1}\right] = \frac{\sqrt{A_i}\mathscr{K}_{P_i+1}\left(\sqrt{A_iB_i}\right)}{\sqrt{B_i}\mathscr{K}_{P_i}\left(\sqrt{A_iB_i}\right)} - \frac{2P_i}{B_i}. \tag{37}$$

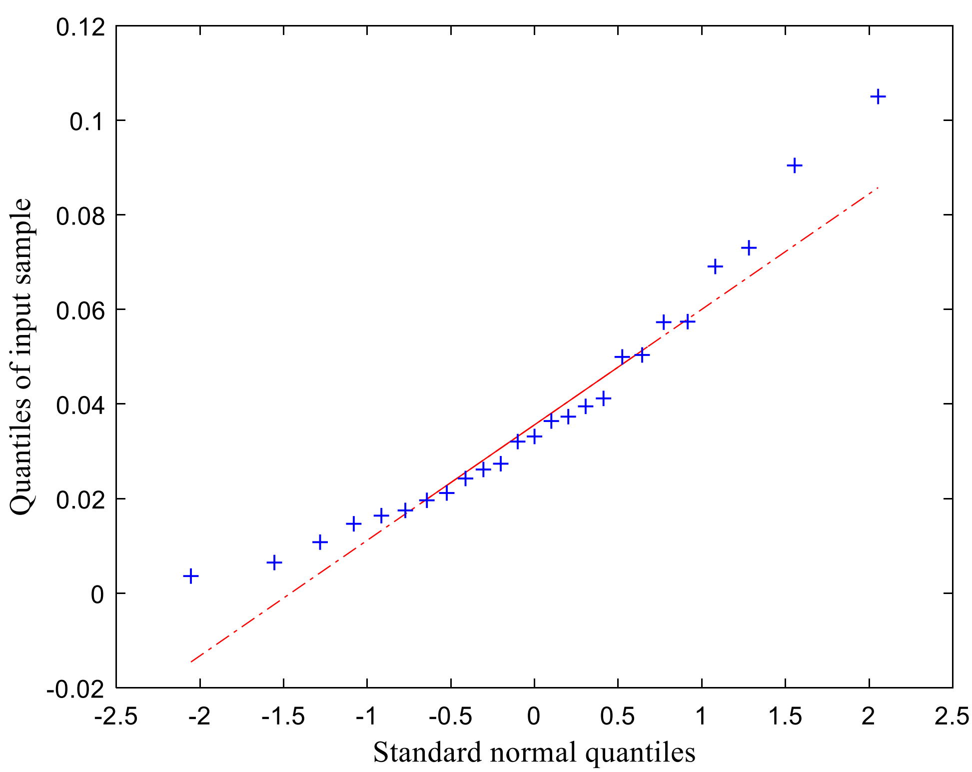

Fig. 3. Q-Q plot of the estimated drift rates versus standard normal distribution.

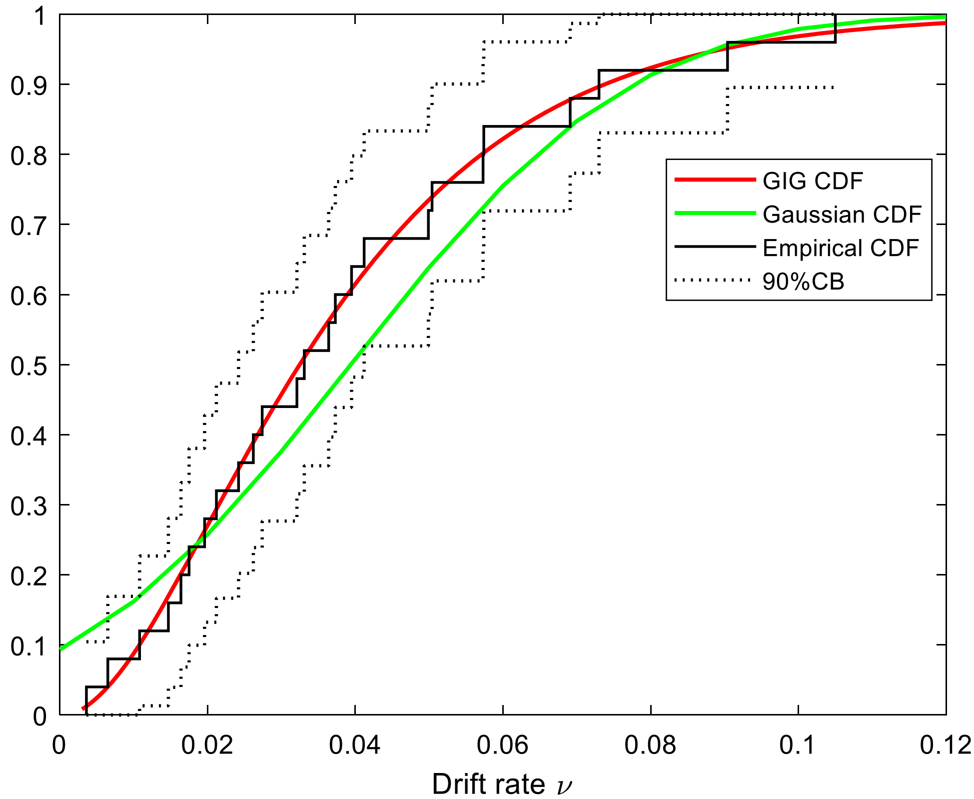

Fig. 4. The CDF for the fitted GIG distribution, the CDF of the fitted normal distribution and the empirical CDF with 90% confidence band (CB) for $\hat{\nu}_i$.

In the prognostics and health management, it pays considerable attention to the degradation rate conditional on the measured degradation signals [33]. Based on (35), we can utilized the online measured degradation observations to update the conditional distribution of the drift rate and the operational status of the in-service units can be monitored periodically.

In the end, the complete algorithm for the model parameters estimation is summarized in **Algorithm 1**.

Algorithm 1*:* Maximum likelihood estimation with EM algorithm
Input: $\mathbf{X} = \{X_1, \ldots, X_n\}$;
1. Initialize the estimates $\mathbf{\Theta}^{(0)}$, $k = 0$;
2. Let $k = k + 1$*:*
E-step: Calculate conditional expectation of $\ell(\mathbf{\Theta}|\mathbf{V}, \mathbf{X})$by using (26)
M-step: Update parameters by using (27)
3. If the difference between the estimates in two consecutive steps is smaller than a predetermined tolerance, then stop. Otherwise, go to Step 2.
Output: ML estimates $\widehat{\Theta}$.

3.3. Interval estimation

The interval estimates for model parameters can be obtained by normal asymptotics. Nevertheless, the observed information matrix is difficult to calculate due to the existence of the modified Bessel function of the second kind. Therefore, we propose to use the parametric bootstrap method for interval estimation. Based on the estimates $\widehat{\Theta}$, we generate the analogues of the degradation data $\mathbf{X}$ and obtain the resample of $\widehat{\Theta}$ by applying the EM algorithm. This process is repeated M times and we get M resamples for the ML estimates : $\{\widehat{\Theta}_1^*, \ldots, \widehat{\Theta}_M^*\}$. Subsequently, the confidence intervals for each parameter can be constructed by calculating the percentiles from $\{\widehat{\Theta}_1^*, \ldots, \widehat{\Theta}_M^*\}$. The algorithm for the bootstrap method is listed in **Algorithm 2**.

Algorithm 2: Bootstrap method for interval estimation
Input: ML estimates $\widehat{\Theta}$;
For s= 1 to M:
1. Generate drift rates ν_i, $i = 1, \ldots, n$ from the GIG distribution $\mathscr{GIG}(\widehat{a}, \widehat{b}, \widehat{p})$.
2. Generate the degradation data $X_i = \{X_{i,1}, \ldots, X_{i,j}\}$ for each unit at $\{t_{1,1}, \ldots, t_{1,m_i}\}$ from the following Wiener process
$X_i(t) = \nu_i \Lambda(t) + \widehat{\kappa}\mathscr{B}(\nu_i \widehat{\Lambda}(t))$.
3. Obtain the ML estimates $\widehat{\Theta}_s^*$ base on the EM algorithm.
Output: M resamples $\{\widehat{\Theta}_1^*, \ldots, \widehat{\Theta}_M^*\}$ for the ML estimates.

4. Illustrative examples

4.1. Application to the IRLEDs degradation data

In this section, the IRLEDs degradation data from Yang [34] is used to validate the proposed model. Under the testing condition of 170 mA, the degradation of IRLEDs increases over time. The IRLEDs are deemed failed when the degradation level exceeds a given threshold. The dataset contains the degradation data of 25 testing samples, where each unit is measured at 11 test time points $\{24, 48, 96, \ldots, 2550\}$. The degradation paths of the 25 units are illustrated in Fig. 1.

From the above figure, we can observe that the degradation rates of the 25 units exhibit an obvious dispersion. To verify the random-effects in the degradation rates, we first fit each degradation path using a basic Wiener process model $X(t) = \nu\Lambda(t) + \sigma\mathscr{B}(\Lambda(t))$. Since the degradation paths appear non-linear, we consider a power law function $\Lambda(t) = t^\theta$ as the transformed time scale.

The histogram of the estimated drift rates for the 25 units is given in Fig. 2. As shown in the figure, the estimated drift rates appear to be right-skewed. To validate this observation, a Q-Q plot of the estimated drift rates versus the standard normal distribution is given in Fig. 3. The

Table 1
Log-likelihood values for the proposed model with different transformed time scales when fitting to the IRLEDs data.

	Power law $\Lambda(t) = t^\theta$	Exponential $\Lambda(t) = \exp(\theta t) - 1$	Logarithm $\Lambda(t) = \ln(\theta t + 1)$
Log-likelihood	−446.18	−498.20	−478.45

Table 2
ML estimates for the parameters in our proposed model when fitting the IRLEDs data.

	θ	a	b	p	κ^2
ML estimates	0.7618	128.4391	6.3454×10^{-5}	2.4375	1.4275
SD	0.0228	5.6098	3.8035×10^{-6}	0.1023	0.2430

Q-Q plot shows a convex curvature, which indicates that the random drift is right-skewed. Therefore, it is reasonable to exploit a skewed distribution, such as the GIG distribution to capture the heterogeneities in the degradation rates.

To check possible correlations between the drift rate and the diffusion coefficient, we calculate the correlation coefficient between $\widehat{v}_i$ and $\widehat{\sigma}_i^2, i = 1, \ldots, 25$, which is 0.9594. This indicates that the drift rate is highly correlated with the diffusion coefficient. Therefore, we consider the following fixed-effects model by imposing $\sigma^2 = \kappa_{ts}^2 v$ to fit the degradation data:

$$X_i(t) = v_i \Lambda(t) + \kappa_{ts} \mathscr{B}(v_i \Lambda(t)). \tag{38}$$

The ML estimates for v_i and κ_{ts}^2 can be obtained as follows after some algebra

$$\widehat{\kappa_{ts}^2} = \frac{1}{\sum_{i=1}^{n} m_i} \sum_{i=1}^{n} \left(\sum_{j=1}^{m_i} \frac{\Delta X_{i,j}^2}{\Delta \Lambda_j} \widehat{v}_i^{\,-1} - 2X_{i,m} + \widehat{v}_i \Lambda_m \right), \tag{39}$$

$$\widehat{v}_i = \frac{1}{2\Lambda_{i,m_i}} \left(\sqrt{m_i{}^2 \widehat{\kappa_{ts}^4} + 4\Lambda_{i,m_i} \sum_{j=1}^{m_i} \frac{\Delta X_{i,j}^2}{\Delta \Lambda_{i,j}}} - m_i \widehat{\kappa_{ts}^2} \right), \ i = 1, \ \ldots, \ 25. \tag{40}$$

Subsequently, a $\mathscr{GIG}(a_{ts}, b_{ts}, p_{ts})$ distribution is employed to fit the ML estimates $\widehat{v}_i$, $i = 1, \ldots, 25$, and the estimates for a_{ts}, b_{ts} *and* p_{ts} are: $\widehat{a}_{ts} = 109.0382$, $\widehat{b}_{ts} = 0.0005$, $\widehat{p}_{ts} = 2.0806$.

The empirical distribution function of $\widehat{v}_i$ and the CDF for $\mathscr{GIG}(\widehat{a}_{ts}, \widehat{b}_{ts}, \widehat{p}_{ts})$ from the estimated GIG distribution are given in Fig. 4. For comparison, we also fit $\widehat{v}_i$ using a normal distribution and the estimated CDF is also given in Fig. 4. As can be seen from the figure, the estimated distribution $\mathscr{GIG}(\widehat{a}_{ts}, \widehat{b}_{ts}, \widehat{p}_{ts})$ agrees well with the empirical distribution, which indicates a good fit for the heterogeneous drift rates in the IRLEDs degradation data.

Thus, there does exist a high positive correlation between the drift rate and diffusion coefficient for IRLEDs in the same batch, and a GIG distribution can provide a good fit for the heterogeneous degradation rates. Based on the above analysis, the proposed random-effects Wiener process model (1) is utilized to fit the IRLEDs degradation data. To verify the assumption on the power-law degradation trend, we also consider (a) the exponential law function $\Lambda(t) = \exp(\theta t) - 1$; and (b) the logarithm form function $\Lambda(t) = \ln(\theta t + 1)$ that are commonly used in engineering practices [22] . Table 1 displays the log-likelihood values for the proposed model with different transformed time scales $\Lambda(t)$. As can be seen from this table, the power law function, i.e. $\Lambda(t) = t^\theta$, provides the best fit for the degradation data.

The detailed estimates for model parameters in the proposed model with power law $\Lambda(t)$ are given in Table 2, where the standard deviations (SD) are obtained by the parametric bootstrap with $M = 1000$ resamples. For the power law $\Lambda(t)$, we note that the estimate of θ is less than 1.

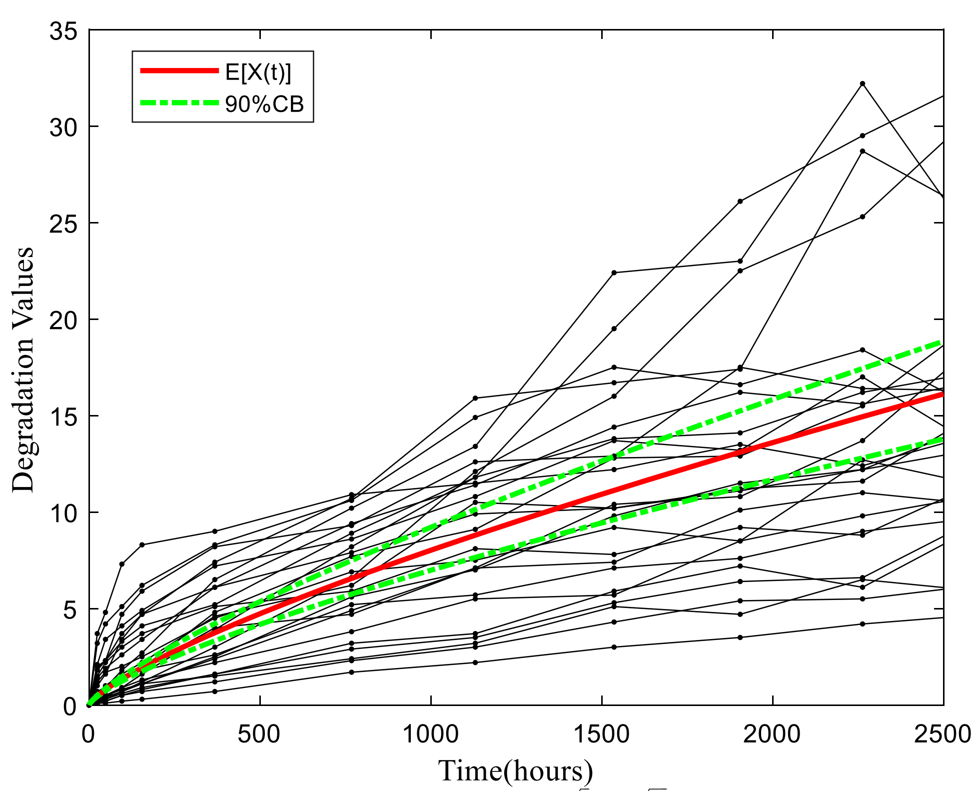

Fig. 5. The expected degradation path $E[X(t)] = \frac{\sqrt{\widehat{b}}\mathscr{K}_{\widehat{p}+1}(\sqrt{\widehat{a}\widehat{b}})}{\sqrt{\widehat{a}}\mathscr{K}_{\widehat{p}}(\sqrt{\widehat{a}\widehat{b}})}\widehat{\Lambda}(t)$ for 25 IRLEDs.

Table 3
The estimation results for our proposed model and its derivative models when fitting the IRLEDs data.

	GIG random-effects model	IG random-effects model	Gamma random-effects model
θ	0.7618	0.7575	0.7617
SD	0.0228	0.0594	0.0522
a	128.4391	45.2929	128.4083
SD	5.6098	4.4429	7.0589
b	6.3454×10^{-5}	0.0699	\
SD	3.8035×10^{-6}	0.0022	\
p	2.4375	\	2.4410
SD	0.1023	\	0.4302
κ^2	1.4275	1.4165	1.3979
SD	0.2430	0.3209	0.2732
Log-likelihood	−446.18	−447.31	−446.17
AIC	902.35	902.61	900.35

This indicates that the degradation of the IRLEDs exhibits a decreasing rate. This is consistent with the degradation patterns in Fig. 1.

The estimate for the expected degradation path $\mathrm{E}[X(t)] = \frac{\sqrt{\hat{b}}\mathscr{K}_{\hat{p}+1}(\sqrt{\hat{a}\hat{b}})}{\sqrt{\hat{a}}\mathscr{K}_{\hat{p}}(\sqrt{\hat{a}\hat{b}})}\widehat{\Lambda}(t)$ and the piecewise confidence band (CB) by bootstrap for the IRLED is illustrated in Fig. 5. As shown in the figure, the expected degradation path properly reflects the degradation pattern of the population.

To further justify the proposed model, we also consider two special cases of the GIG random-effects model to model the heterogeneities, i.e., the IG random-effects model and the Gamma random-effects model. The IG random-effects model can be obtained by fixing $p = -1/2$ in the proposed model, while the Gamma random-effects model is obtained by fixing $b = 0$. The estimation results for our proposed model and its special cases are listed in Table 3, where the estimates are obtained from the EM algorithm and the standard deviations (SD) are obtained from the parametric bootstrap with $M = 1000$ resamples. The log-likelihood value and the AIC value are given for each model. From the table, we can note that the Gamma random-effects model has a very close log-likelihood value to the more general GIG random-effects model, and the AIC value of the Gamma random-effects model is the smallest. This implies that the Gamma random-effects model may be more suitable for the IRLEDs dataset.

4.2. Application to the GaAs laser device degradation data

To further investigate the performance of the proposed model on real degradation data, the GaAs laser degradation data from Meeker and Escobar [35] is fitted by the proposed GIG model. This dataset contains the degradation measurements from 15 testing samples of laser devices, each of which is measured at times $\{250, 500, \ldots, 4000\}$. The

Table 4
The log-likelihood values and AIC values for different models when fitted to the laser devices data.

		Log-likelihood	AIC
Linear	GIG random-effects model	74.09	−140.17
	IG random-effects model	74.08	−142.16
	Gamma random-effects model	73.79	−141.58
Power law	GIG random-effects model	74.09	−138.19
	IG random-effects model	74.09	−140.18
	Gamma random-effects model	73.80	−139.60
Existing models	Gaussian drift model [22]	69.19	−132.38
	Skew-normal drift model [36]	71.11	−134.22
	Normal-Gamma drift-volatility [26]	72.86	−137.73

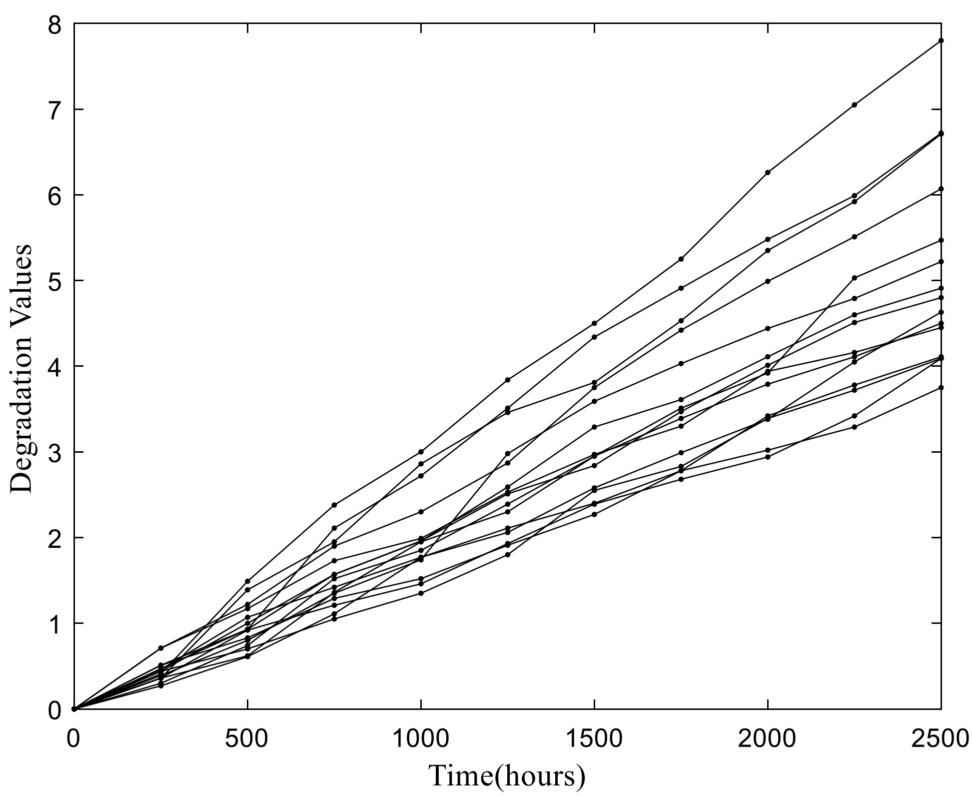

Fig. 6. Degradation paths of 15 laser devices.

degradation paths of 15 laser devices are plotted in Fig. 6.

From Fig. 6, it can be noticed that the degradation paths of 15 laser devices appear to have a linear trend with time. Therefore, we utilize both linear and power law degradation trend, namely $\Lambda(t) = t$ and $\Lambda(t) = t^{\theta}$, to model the degradation paths. In Table 4, the performance of the proposed model and its two special cases are summarized for the linear and power law cases. Different from the IRLEDs case, the IG random-effects model exhibits a better performance than the GIG random-effects model and the Gamma random-effects model for the laser device dataset according to the AIC values.

According to the results in [29], the dataset was also fitted by the following three models: (a) the commonly used random-effects Wiener process model with Gaussian drift [22]; (b) the random-effects Wiener process model with skew-normal drift [36]; (c) the random-effects Wiener process model with normal-Gamma drift-volatility [26]. To ease the reference, we also list these results in Table 4. As can be noted, the proposed models have better performance than these existing models in terms of the log-likelihood values and AIC values.

5. Conclusions

Degradation modeling plays an important role in reliability assessment. In this study, we proposed a general random-effects Wiener process model to capture the unit-to-unit heterogeneities in the degradation. We used a Wiener process model to characterize the degradation of each unit, and a GIG distribution to capture the heterogeneous degradation rates in the population. The proposed model includes the existing IG random-effects Wiener process model in [29] as a special case, and also introduces a useful special case, i.e., the Gamma random-effects Wiener process model.

The proposed model was applied to an IRLEDs dataset and a laser device dataset to show its applicability. For the IRLEDs dataset, the Gamma random-effects model outperforms the more general GIG random-effects model and the IG random-effects model in terms of the AIC criterion. For the laser device dataset, the IG random-effects model performs the best and outperforms the existing models, such as the widely used Gaussian drift model and the complicated Normal-Gamma drift-volatility model. The application of the proposed model to the real degradation datasets indicates that the GIG random-effects model, including two of its special cases, have a satisfactory performance in reality.

Further studies can be carried out based on the results of this paper. One possible research direction for future studies is to extend the proposed model to accelerated degradation test, and investigate the design for the optimal test schemes based on this type of models. In addition, it is worthwhile to consider the optimal maintenance strategies for products subject to degradation, where the degradation process is characterized by the proposed model.

Declaration of Competing Interest

No

Acknowledgment

This work is supported in part by the Natural Science Foundation of China under the grant 71901138.

References

[1] Zhai Q, Ye Z-S. Degradation in common dynamic environments. Technometrics 2018;60(4):461–71.
[2] Ahmad W, Khan SA, Islam MMM. A reliable technique for remaining useful life estimation of rolling element bearings using dynamic regression models. Reliab Eng Syst Saf 2019;184:67–76.
[3] Hu J, Chen P. Predictive maintenance of systems subject to hard failure based on proportional hazards model. Reliab Eng Syst Saf 2020;196:106707.
[4] Wen Y, Wu J, Yuan Y. Multiple-phase modeling of degradation signal for condition monitoring and remaining useful life prediction. IEEE Trans Reliab 2017;66(3):924–38.
[5] Wu J, Guo P, Cheng Y. Ensemble generalized multiclass support-vector-machine-based health evaluation of complex degradation systems. IEEE-Asme Trans Mechatron 2020;25(5):2230–40.
[6] Peng W, Ye Z, Chen N. Bayesian deep-learning-based health prognostics toward prognostics uncertainty. IEEE Trans Ind Electron 2020;67(3):2283–93.
[7] Zhou S, Xu A. Exponential dispersion process for degradation analysis. IEEE Trans Reliab 2019;68(2):398–409.
[8] Peng W, Ye Z, Chen N. Joint online RUL prediction for multivariate deteriorating systems. IEEE Trans Ind Inf 2019;15(5):2870–8.
[9] Zhai Q, Ye Z. RUL prediction of deteriorating products using an adaptive Wiener process model. IEEE Trans Ind Inf 2017;13(6):2911–21.
[10] Xiao X, Ye Z. Optimal design for destructive degradation tests with random initial degradation values using the Wiener process. IEEE Trans Reliab 2016;65(3):1327–42.
[11] Wen Y, Wu J, Das D. Degradation modeling and RUL prediction using Wiener process subject to multiple change points and unit heterogeneity. Reliab Eng Syst Saf 2018;176:113–24.
[12] Sun Q, Ye Z, Hong Y. Statistical modeling of multivariate destructive degradation tests with blocking. Technometrics 2020;62(4):536–48.
[13] Zhao X, He K, Kuo W. Planning accelerated reliability tests for mission-oriented systems subject to degradation and shocks. IISE Trans 2020;52(1):91–103.
[14] Chatenet Q, Remy E, Gagnon M. Modeling cavitation erosion using non-homogeneous gamma process. Reliab Eng Syst Saf 2021;213:107671.
[15] Peng W, Li Y, Yang Y. Bayesian degradation analysis with inverse Gaussian process models under time-varying degradation rates. IEEE Trans Reliab 2017;66(1):84–96.
[16] Xu A, Hu J, Wang P. Degradation modeling with subpopulation heterogeneities based on the inverse Gaussian process. Appl Math Modell 2020;81:177–93.
[17] Dong Q, Cui L, Si S. Reliability and availability analysis of stochastic degradation systems based on bivariate Wiener processes. Appl Math Modell 2020;79:414–33.
[18] Zhang H, Mo Z, Wang J. Nonlinear-drifted fractional Brownian motion with multiple hidden state variables for remaining useful life prediction of Lithium-ion batteries. IEEE Trans Reliab 2020;69(2):768–80.
[19] Wang H, Zhao Y, Ma X. Mechanism equivalence in designing optimum step-stress accelerated degradation test plan under Wiener process. IEEE Access 2018;6:4440–51.
[20] Zhao X, Chen P, Gaudoin O. Accelerated degradation tests with inspection effects. Eur J Oper Res 2021;292(3):1099–114.
[21] Li H, Pan D, Chen CLP. Reliability modeling and life estimation using an expectation maximization based Wiener degradation model for momentum wheels. IEEE Transactions on Cybernetics 2015;45(5):955.
[22] Ye ZS, Wang Y, Tsui KL. Degradation data analysis using Wiener processes with measurement errors. IEEE Trans Reliab 2013;62(4):772–80.
[23] Sun L, Balakrishnan N, Zhao F. Mis-specification analysis of the impact of covariates on the diffusion coefficient in Wiener degradation process. Commun Stat - Simul Comput 2020:1–19.
[24] Sun F, Fu F, Liao H. Analysis of multivariate dependent accelerated degradation data using a random-effect general Wiener process and D-vine Copula. Reliab Eng Syst Saf 2020;204:107168.
[25] Xu X, Tang S, Yu C. Remaining useful life prediction of Lithium-ion batteries based on Wiener process under time-varying temperature condition. Reliab Eng Syst Saf 2021:107675.
[26] Wang X. Wiener processes with random effects for degradation data. J Multivar Anal 2010;101(2):340–51.
[27] Ye Z, Chen N, Shen Y. A new class of Wiener process models for degradation analysis. Reliab Eng Syst Saf 2015;139:58–67.
[28] Tang S, Yu C, Wang X. Remaining useful life prediction of Lithium-ion batteries based on the Wiener process with measurement error. Energies 2014;7(2):520–47.
[29] Zhai Q, Chen P, Hong L. A random-effects Wiener degradation model based on accelerated failure time. Reliab Eng Syst Saf 2018;180:94–103.
[30] Yan B, Ma X, Yang L. A novel degradation-rate-volatility related effect Wiener process model with its extension to accelerated ageing data analysis. Reliab Eng Syst Saf 2020;204:107138.
[31] Jorgensen B. Statistical properties of the generalized inverse Gaussian distribution. Springer-Verlag; 1982.
[32] Chen P, Ye Z-S. Estimation of field reliability based on aggregate lifetime data. Technometrics 2017;59(1):115–25.
[33] Wen Y, Wu J, Zhou Q. Multiple-change-point modeling and exact Bayesian inference of degradation signal for prognostic improvement. IEEE Trans Autom Sci Eng 2019;16(2):613–28.
[34] Yang G. Life cycle reliability engineering. New Jersey: John Wiley & Sons; 2007.
[35] Meeker WQ, Escobar L. Statistical *methods for reliability data*, New York. John Wiley & Sons; 1998.
[36] Peng CY, Tseng ST. Statistical lifetime inference with skew-Wiener linear degradation models. IEEE Trans Reliab 2013;62(2):338–50.